

# Linear and nonlinear dynamics of matter wave packets in periodic potentials

Th. Anker, M. Albiez, B. Eiermann, M. Taglieber and M. K. Oberthaler

*Kirchhoff Institut für Physik, Universität Heidelberg, Im Neuenheimer Feld 227, 69120 Heidelberg*

[thomas.anker@kip.uni-heidelberg.de](mailto:thomas.anker@kip.uni-heidelberg.de)

<http://www.kip.uni-heidelberg.de/matterwaveoptics>

## Abstract

We investigate experimentally and theoretically the nonlinear propagation of  $^{87}\text{Rb}$  Bose Einstein condensates in a trap with cylindrical symmetry. An additional weak periodic potential which encloses an angle with the symmetry axis of the waveguide is applied. The observed complex wave packet dynamics results from the coupling of transverse and longitudinal motion. We show that the experimental observations can be understood applying the concept of effective mass, which also allows to model numerically the three dimensional problem with a one dimensional equation. Within this framework the observed slowly spreading wave packets are a consequence of the continuous change of dispersion. The observed splitting of wave packets is very well described by the developed model and results from the nonlinear effect of transient solitonic propagation.

---

## References and links

1. "Bose-Einstein condensation in atomic gases", ed. by M. Inguscio, S. Stringari, and C. Wieman, (IOS Press, Amsterdam 1999)
2. F.S. Cataliotti, S. Burger, S. C. Fort, P. Maddaloni, F. Minardi, A. Trombettoni, A. Smerzi, and M. Inguscio, "Josephson Junction Arrays with Bose-Einstein Condensates", *Science* **293** 843 (2001).
3. A. Trombettoni and A. Smerzi, "Discrete Solitons and Breathers with Dilute Bose-Einstein Condensates", *Phys. Rev. Lett.* **86** 2353 (2001).
4. M. Steel and W. Zhang, "Bloch function description of a Bose-Einstein condensate in a finite optical lattice", *cond-mat/9810284* (1998).
5. P. Meystre, "Atom Optics" (Springer Verlag, New York, 2001) p 205, and references therein.
6. The experimental realization in our group will be published elsewhere.
7. V.V. Konotop, M. Salerno, "Modulational instability in Bose-Einstein condensates in optical lattices", *Phys. Rev. A* **65** 021602 (2002).
8. N. Ashcroft and N. Mermin, "Solid State Physics" (Saunders, Philadelphia, 1976).
9. A.A. Sukhorukov, D. Neshev, W. Krolikowski, and Y.S. Kivshar, "Nonlinear Bloch-wave interaction and Bragg scattering in optically-induced lattices", *nlin.PS/0309075*.
10. B. Eiermann, P. Treutlein, Th. Anker, M. Albiez, M. Taglieber, K.-P. Marzlin, and M.K. Oberthaler, "Dispersion Management for Atomic Matter Waves", *Phys.Rev.Lett.* **91** 060402 (2003).
11. M. Kozuma, L. Deng, E.W. Hagley, J. Wen, R. Lutwak, K. Helmerson, S.L. Rolston, and W.D. Phillips, "Coherent Splitting of Bose-Einstein Condensed Atoms with Optically Induced Bragg Diffraction", *Phys.Rev.Lett.* **82** 871 (1999).
12. B.P. Anderson, and M.A. Kasevich, "Macroscopic Quantum Interference from Atomic Tunnel Arrays", *Science* **282** 1686 (1998);
13. O. Morsch, J. Müller, M. Cristiani, D. Ciampini, and E. Arimondo, "Bloch Oscillations and Mean-Field Effects of Bose-Einstein Condensates in 1D Optical Lattices", *Phys. Rev. Lett.* **87** 140402 (2001).
14. C.F. Bharucha, K.W. Madison, P.R. Morrow, S.R. Wilkinson, Bala Sundaram, and M.G. Raizen, "Observation of atomic tunneling from an accelerating optical potential", *Phys.Rev. A* **55** R857 (1997)

15. L. Salasnich, A. Parola, and L. Reatto, "Effective wave equations for the dynamics of cigar-shaped and disk-shaped Bose condensates", *Phys. Rev. A* **65** 043614 (2002).
  16. G.P. Agrawal, "Applications of Nonlinear Fiber Optics" (Academic Press, San Diego, 2001). G.P. Agrawal, "Nonlinear Fiber Optics" (Academic Press, San Diego, 1995).
  17. R.G. Scott, A.M. Martin, T.M. Fromholz, S. Bujkiewicz, F.W. Sheard, and M. Leadbeater, "Creation of Solitons and Vortices by Bragg Reflection of Bose-Einstein Condensates in an Optical Lattice", *Phys. Rev. Lett.* **90** 110404 (2003).
- 

## 1. Introduction

The experimental investigation of nonlinear matter wave dynamics is feasible since the realization of Bose-Einstein-condensation of dilute gases [1]. The combination of this new matter wave source with periodic potentials allows for the realization of many nonlinear propagation phenomena. The dynamics depends critically on the modulation depth of the potential. For deep periodic potentials the physics is described locally taking into account mean field effects and tunneling between adjacent potential wells. In this context wave packet dynamics in Josephson junction arrays have been demonstrated experimentally [2] and nonlinear self trapping has been predicted theoretically [3]. In the limit of weak periodic potentials and moderate nonlinearity rich wave packet dynamics result due to the modification of dispersion which can be described applying band structure theory [4]. Especially matter wave packets subjected to anomalous dispersion (negative effective mass) or vanishing dispersion (diverging mass) are of great interest. In the negative mass regime gap solitons have been predicted theoretically [5] and have been observed recently [6]. Also modulation instabilities can occur [7].

The experiments described in this work reveal wave dynamics in the linear and nonlinear regime for weak periodic potentials. The observed behavior is a consequence of the special preparation of the wave packet leading to a continuous change of the effective mass and thus the dispersion during the propagation. The initial propagation is dominated by the atom-atom interaction leading to complex wave dynamics. After a certain time of propagation slowly spreading atomic wave packets are formed which are well described by linear theory. In this work we focus on the mechanisms governing the initial stage of propagation.

The paper is organized as follows: in section 2 we describe the effective mass and dispersion concept. In section 3 we present our experimental setup and in section 4 the employed wave packet preparation schemes are discussed in detail. In section 5 the experimental results are compared with numerical simulations. We show that some features of the complex dynamics can be identified with well known nonlinear mechanisms. We conclude in section 6.

## 2. Effective mass and dispersion concept

In our experiments we employ a weak periodic potential which leads to a dispersion relation  $E_n(q)$  shown in Fig. 1(a). This relation is well known in the context of electrons in crystals [8] and exhibits a band structure. It shows the eigenenergies of the Bloch states as a function of the quasi-momentum  $q$ . The modified dispersion relation leads to a change of wavepacket dynamics due to the change in group velocity  $v_g(q) = 1/\hbar \partial E/\partial q$  (see Fig. 1(b)), and the group velocity dispersion described by the effective mass  $m_{eff} = \hbar^2(\partial^2 E/\partial q^2)^{-1}$  (see Fig. 1(c)), which is equivalent to the effective diffraction introduced in the context of light beam propagation in optically-induced photonic lattices [9]. In our experiment only the lowest band is populated, which is characterized by two dispersion regimes, normal and anomalous dispersion, corresponding to positive and negative effective mass. A pathological situation arises at the quasimomentum  $q_\infty^\pm$ , where the group velocity  $v_g(q)$  is extremal,  $|m_{eff}|$  diverges and thus the dispersion vanishes.

In the following we will show that the two preparation schemes employed in the experi-

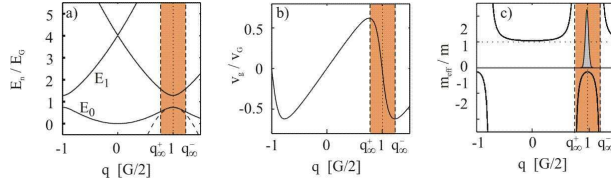


Fig. 1. (a) Band structure for atoms in an optical lattice with  $V_0 = 1.2E_{rec}$  (solid), parabolic approximation to the lowest energy band at  $q = \pi/d = G/2$  (dashed), corresponding group velocity (b) and effective mass (c) in the lowest energy band. The vertical dashed lines at  $q = q_{\infty}^{\pm}$  indicate where  $|m_{\text{eff}}| = \infty$ . The shaded region shows the range of quasimomenta where the effective mass is negative.

ment lead to a continuous change of the quasimomentum distribution, and thus to a continuous change of dispersion. One of the preparation schemes allows to switch periodically from positive to negative mass values and thus a slowly spreading wave packet is formed. This is an extension of the experiment reporting on dispersion management [10]. The second preparation gives further insight into the ongoing nonlinear dynamics for the initial propagation.

### 3. Experimental Setup

The wave packets in our experiments have been realized with a  $^{87}\text{Rb}$  Bose-Einstein condensate (BEC). The atoms are collected in a magneto-optical trap and subsequently loaded into a magnetic time-orbiting potential trap. By evaporative cooling we produce a cold atomic cloud which is then transferred into an optical dipole trap realized by two focused Nd:YAG laser beams with  $60\ \mu\text{m}$  waist crossing at the center of the magnetic trap (see Fig.2(a)). Further evaporative cooling is achieved by lowering the optical potential leading to pure Bose-Einstein condensates with  $1 \cdot 10^4$  atoms in the  $|F = 2, m_F = +2\rangle$  state. By switching off one dipole trap beam the atomic matter wave is released into a trap acting as a one-dimensional waveguide with radial trapping frequency  $\omega_{\perp} = 2\pi \cdot 100\ \text{Hz}$  and longitudinal trapping frequency  $\omega_{\parallel} = 2\pi \cdot 1.5\ \text{Hz}$ . It is important to note that the dipole trap allows to release the BEC in a very controlled way leading to an initial mean velocity uncertainty smaller than  $1/10$  of the photon recoil velocity.

The periodic potential is realized by a far off-resonant standing light wave with a single beam peak intensity of up to  $1\ \text{W}/\text{cm}^2$ . The chosen detuning of  $2\ \text{nm}$  to the blue off the D2 line leads to a spontaneous emission rate below  $1\ \text{Hz}$ . The standing light wave and the waveguide enclose an angle of  $\theta = 21^\circ$  (see Fig. 2(b)). The frequency and phase of the individual laser beams are controlled by acousto-optic modulators driven by a two channel arbitrary waveform generator allowing for full control of the velocity and amplitude of the periodic potential. The light intensity and thus the absolute value of the potential depth was calibrated independently by analyzing results on Bragg scattering [11] and Landau Zener tunneling [12, 13, 14].

The wave packet evolution inside the combined potential of the waveguide and the lattice is studied by taking absorption images of the atomic density distribution after a variable time delay. The density profiles along the waveguide,  $n(x, t)$ , are obtained by integrating the absorption images over the transverse dimension.

### 4. Dynamics in reciprocal space

In our experimental situation an acceleration of the periodic potential to a constant velocity leads to a collective transverse excitation as indicated in Fig. 2(d). Since the transverse motion in the waveguide has a non vanishing component in the direction of the periodic potential due to the angle  $\theta$ , a change of the transverse velocity leads to a shift of the central quasimomentum of

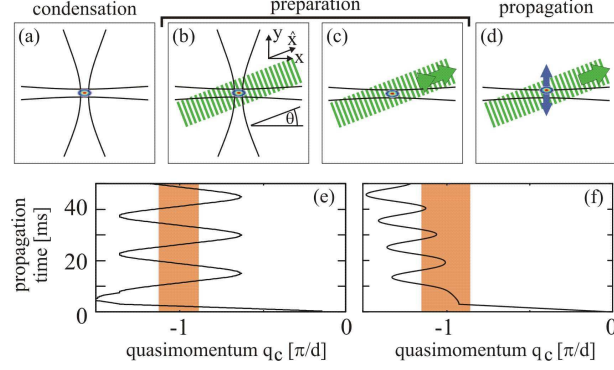


Fig. 2. Scheme for wave packet preparation (a-d). (a) initial wave packet is obtained by condensation in a crossed dipole trap. (b) A stationary periodic potential is ramped up adiabatically preparing the atoms at quasimomentum  $q_c = 0$  in the lowest band. (c),(d) The periodic potential is accelerated to a constant velocity. (e) shows the numerically deduced quasimomentum shift for the preparation method I described in the text. (f) The motion of the center quasimomentum for the preparation method II described in the text. The additional shift to higher quasimomenta for long times results from the residual trap in the direction of the waveguide. The shaded area represents the quasimomenta corresponding to negative effective mass.

the wave packet. The coupling between the transverse motion in the waveguide and the motion along the standing light wave gives rise to a nontrivial motion in reciprocal (see Fig. 2(e,f)) and real space.

The appropriate theoretical description of the presented experimental situation requires the solution of the three dimensional nonlinear Schrödinger equation (NLSE) and thus requires long computation times. In order to understand the basic physics we follow a simple approach which solves the problem approximately and explains all the features observed in the experiment. For that purpose we first solve the semiclassical equations of motion of a particle which obeys the equation  $\vec{F} = M^* \ddot{\vec{x}}$  where  $M^*$  is a mass tensor describing the directionality of the effective mass. We deduce the time dependent quasimomentum  $q_c(t)$  in the direction of the periodic potential by identifying  $\hbar q_c = F_{\hat{x}}$  and  $\hat{x} = v_g(q_c)$  (definition of  $\hat{x}$  see Fig. 2(b)). Subsequently we can solve the one dimensional NPSE (non-polynomial nonlinear Schrödinger equation)[15] where the momentum distribution is shifted in each integration step according to the calculated  $q_c(t)$ . Thus the transverse motion is taken into account properly for *narrow* momentum distributions. We use a split step Fourier method to integrate the NPSE where the kinetic energy contribution is described by the numerically obtained energy dispersion relation of the lowest band  $E_0(q)$ . It is important to note, that this description includes all higher derivatives of  $E_0(q)$ , and thus goes beyond the effective mass approximation.

In the following we discuss in detail the employed preparation schemes:

*Acceleration scheme I:* After the periodic potential is adiabatically ramped up to  $V_0 = 6E_{rec}$  it is accelerated within 3 ms to a velocity  $v_{pot} = \cos^2(\theta)1.5v_{rec}$ . Then the potential depth is lowered to  $V_0 = 0.52E_{rec}$  within 1.5 ms and the periodic potential is decelerated within 3 ms to  $v_{pot} = \cos^2(\theta)v_{rec}$  subsequently.  $V_0$  and  $v_{pot}$  are kept constant during the following propagation. The calculated motion in reciprocal space  $q_c(t)$  is shown in Fig. 2(e).

*Acceleration scheme II:* The periodic potential is ramped up adiabatically to  $V_0 = 0.37E_{rec}$  and is subsequently accelerated within 3 ms to a final velocity  $v_{pot} = \cos^2(\theta) \times 1.05v_{rec}$ . The potential depth is kept constant throughout the whole experiment. Fig. 2(f) reveals that in con-

trast to the former acceleration scheme the quasimomentum for the initial propagation is mainly in the negative effective mass regime.

## 5. Experimental and Numerical Results

In this section we compare the experimental results with the predictions of our simple theoretical model discussed above. The numerical simulation reveal all the experimentally observed features of the dynamics such as linear slowly spreading oscillating wave packets, nonlinear wave packet compression and splitting of wave packets. The observed nonlinear phenomena can be understood by realizing that in the negative effective mass regime the repulsive atom-atom interaction leads to compression of the wave packet in real space and to a broadening of the momentum distribution. An equivalent picture borrowed from nonlinear photon optics [16] is the transient formation of higher order solitons, which show periodic compression in real space with an increase in momentum width and vice versa.

### 5.1. Preparation I

The experimental results for the first acceleration scheme discussed in section 4 are shown in Fig. 3. Clearly we observe that a wave packet with reduced density is formed which spreads out slowly and reveals oscillations in real space. This wave packet results from the initial dynamics characterized by two stages of compression which lead to radiation of atoms [17]. The observed behavior is well described by our numerical simulation which allows further insight into the ongoing physics.

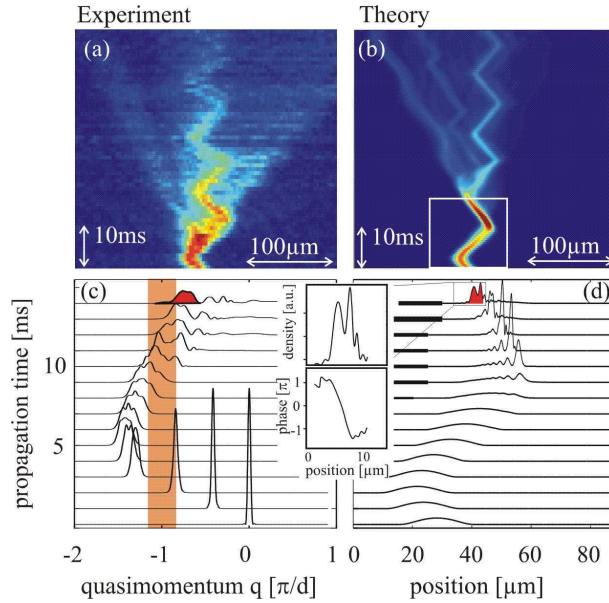


Fig. 3. Wave packet dynamics for preparation I. (a) Experimental observation of wave packet propagation. (b) Result of the numerical simulation as discussed in the text. The data is convoluted with the optical resolution of the experiment. The obtained results are in good agreement with the experimental observations. The theoretically obtained (c) quasimomentum distribution and (d) real space distribution are given for the initial 14ms of propagation. The inset reveals the phase of the observed slowly spreading wave packet.

In Fig. 3(c,d) we show the calculated momentum and real space distribution for the first 14ms

of propagation. As can be seen the acceleration of the standing light wave leads to an oscillatory behavior in momentum space. For the chosen parameters the wave packet is initially dragged with a tight binding potential ( $V_0 = 6E_{rec}$ ) over the critical negative mass regime. While the real space distribution does not change during this process, the momentum distribution broadens due to self phase modulation [16]. The subsequent propagation in the positive mass regime leads to a further broadening in momentum space and real space ( $t=4-9$ ms).

The dynamics changes drastically as soon as a significant part of the momentum distribution populates quasimomenta in the negative mass regime ( $t=10$ ms). There the real space distribution reveals nonlinear compression as known from the initial dynamics of higher order solitons. This compression leads to a significant further broadening in momentum space and thus to population of quasimomenta corresponding to positive mass. This results in a spreading in real space due to the different group velocities involved and leads to the observed background. The change of the quasimomentum due to the transverse motion prohibits a further significant increase in momentum width, since the whole momentum distribution is shifted out of the critical negative mass regime at  $t=14$ ms.

The long time dynamics of the slowly spreading wave packet is mainly given by the momentum distribution marked with the shaded area for  $t=14$ ms in Fig. 3(c). The subsequent motion is dominated by the change of the quasimomentum due to the transverse motion. This leads to a periodic change from normal to anomalous dispersion and thus the linear spreading is suppressed. This is an extension of our previous work on dispersion management for matter waves - continuous dispersion management.

## 5.2. Preparation II

This preparation scheme reveals in more detail the transient solitonic propagation leading to the significant spreading in momentum space. This results in a splitting of the wave packet which cannot be understood within a linear theory. The results are shown in Fig. 4 and the observed splitting is confirmed by our numerical simulations.

In contrast to the former preparation scheme the momentum distribution is prepared as a whole in the critical negative mass regime. Our numerical simulations reveal that the wave packet compresses quickly in real space after  $t=4$ ms which is accompanied by an expansion in momentum space. The momentum distribution which stays localized in the negative mass regime reveals further solitonic propagation characterized by an expansion in real space and narrowing of the momentum distribution ( $t=5-10$ ms). The transverse motion shifts this momentum distribution into the normal dispersion regime after 11ms of propagation resulting in a wave packet moving with positive group velocity (i.e. moving to the right in fig. 4(b)). The initial compression at  $t=4$ ms even produces a significant population of atoms in the normal mass regime which subsequently move with negative group velocity showing up as a wave packet moving to the left in Fig. 4(b). Thus the splitting in real space is a consequence of the significant nonlinear broadening in momentum space.

## 6. Conclusion

In this paper we report on experimental observations of nonlinear wave packet dynamics in the regime of positive and negative effective mass. Our experimental setup realizing a BEC in a quasi-one dimensional situation allows the observation of wave dynamics for short times, where the nonlinearity due to the atom-atom interaction dominates and also for long times, where linear wave propagation is revealed.

We have shown that a slowly spreading wave packet can be realized by changing the quasimomentum periodically from the normal to anomalous dispersion regime. This can be viewed as an implementation of continuous dispersion management. We further investigate in detail

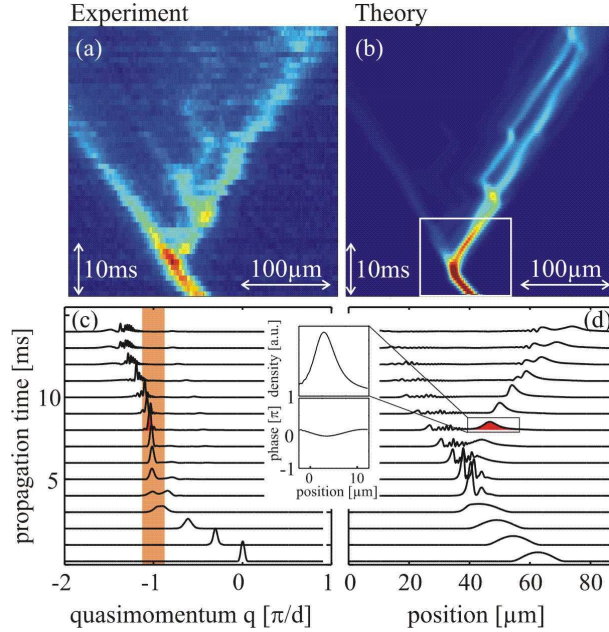


Fig. 4. Wave packet dynamics for preparation II. (a) Experimental results on wave packet propagation. (b) Result of the numerical simulation as discussed in the text. The simulation reproduces the observed wave packet splitting. The theoretically obtained (c) quasimomentum distribution and (d) real space distribution are given for the initial 14ms of propagation. The inset reveals that the transient formed wave packet has a flat phase indicating solitonic propagation.

the formation process of these packets, which are a result of the initial spreading in momentum space due to nonlinear compression. A second experiment investigates in more detail the nonlinear dynamics in the negative mass regime where the solitonic propagation leads to a significant broadening in momentum space. This shows up in the experiment as splitting of the condensate into two wave packets which propagate in opposite directions.

The developed theoretical description utilizing the effective mass tensor models the experimental system in one dimension and can explain all main features observed in the experiment.

## 7. Acknowledgment

This work was supported by Deutsche Forschungsgemeinschaft, Emmy Noether Program, by the European Union, Contract No. HPRN-CT-2000-00125, and the Optik Zentrum University of Konstanz.